NANO
LETTERS

2005
Vol. 5, No. 9
1710−1715

Facile Scheme for Fabricating Solid-State Nanostructures Using E-Beam Lithography and Solution Precursors

Suresh Donthu, Zixiao Pan, Benjamin Myers, Gajendra Shekhawat, Nianqiang Wu, and Vinayak Dravid*

Department of Materials Science and Engineering, 2220 Campus Drive, Northwestern University, Evanston, Illinois 60208

Received May 21, 2005

ABSTRACT

We demonstrate a facile approach for site-specific fabrication of organic, inorganic, and hybrid solid-state nanostructures through a novel combination of electron-beam lithography (eBL) and spin coating of liquid and sol–gel precursors, termed soft eBL. By using eBL patterned resists as masks in combination with a low cost process such as spin coating, directed growth of nanostructures with controlled dimensions is achieved without the need for the costly and difficult process step of etching ceramics. The highly versatile nature of the scheme is highlighted through the fabrication of nanostructures of a variety of materials such as ferroelectric, optoelectronic, and conducting polymeric materials at different length scales and spatial densities on a multitude of substrates.

The ability to manipulate materials at nanometer-length scales and control the dimensions of nanostructures is a prerequisite of not only studing novel properties of materials at different length scales but also of realizing useful miniaturized devices. Nanopatterning of materials is one approach that enables these dual goals. Functional ceramics such as ferroelectric (e.g., $PbZr_xTi_{1-x}O_3$ − PZT), ferromagnetic (e.g., $CoFe_2O_4$ − CFO), and optoelectronic materials (e.g., ZnO) are very important technological materials for applications such as actuators,[1,2] chemical sensors,[3−5] high-density data storage,[6,7] and polychromic displays.[8−10] Some of these properties show remarkable size dependency[11,12] as well as interesting synergistic coupling[13,14] when materials with different functionalities are positioned in close proximity. The ability to create nanoscale architecture for functional ceramics is a prerequisite of exploring the rich field of ceramic nanotechnology.

Although several nanopatterning schemes[15−21] have been developed during the last two decades, techniques that can pattern ceramics under 100-nm resolution are very limited.[22] This is due in part to the refractory nature of ceramics and the difficulty in etching such materials.[2] Dip-pen nanolithography (DPN) with sol−gel inks[16] has been employed to generate structures under 200 nm. Another high-resolution nanopatterning technique for ceramics is the direct-write using an electron beam.[12,23] Although this technique was shown to generate very fine structures (<10 nm), it is limited to resists that are sensitive to e-beams and the process typically requires a high electron dose for development of e-beam-sensitive inorganic resists. Other patterning techniques based on molding and replication[22,24,25] processes generate ceramic structures over fairly large areas, and direct-write fabrication techniques such as robotic deposition of polyelectrolytes could generate 3D ceramic architectures.[26,27] However, these techniques do not attain true nanometer-scale patterning resolution. Here we report a general scheme for fabricating ceramic nanostructures with control over not only their dimensions but also over their location

The critical steps in our patterning scheme are shown schematically in Figure 1. The first step is to sequentially spin-coat the bilayer structure of e-beam resists with a high sensitivity MMA-MAA copolymer (MMA(8.5)MAA EL6) at the bottom and a low sensitivity PMMA (950PMMA A3, from MicroChem) resist on top. The higher sensitivity of the copolymer compared to PMMA affords excellent lift-off. Each layer is spin-coated at 3000 rpm for 45 s to give a nominal thickness of about 150 nm. E-beam resist coated substrates were patterned subsequently at 30kV with line doses between 0.8 and 1.2 nC/cm using Quanta 600F (FEI Co.), which can be operated in variable/high-pressure mode for patterning insulating substrates. The same machine is used for subsequent imaging of the patterns. The patterned substrates were then treated with oxygen plasma for 20 s

* Corresponding author. E-mail: v-dravid@northwestern.edu.

10.1021/nl050954t CCC: $30.25
Published on Web 08/04/2005

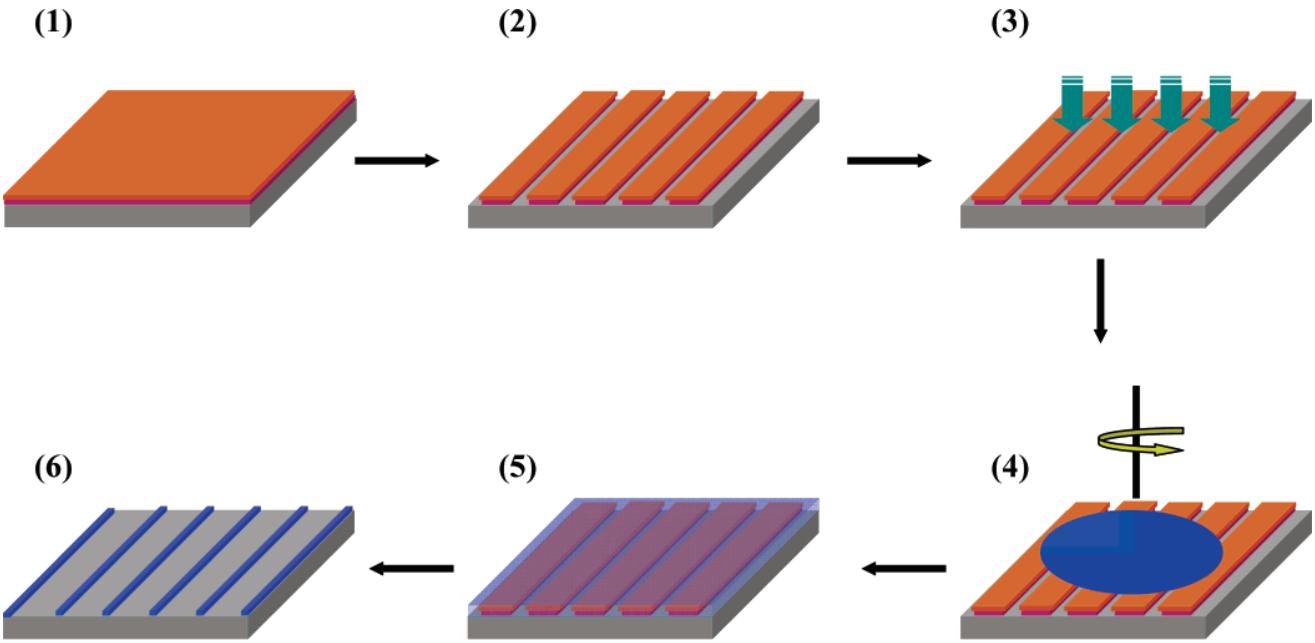

Figure 1. Schematic illustration of the soft eBL patterning scheme. (1) Spin coat PMMA and MMA e-beam sensitive bi-layers, (2) e-beam lithography, (3) treat the patterned substrates under oxygen plasma, (4) deposit the solution and spin the substrate, (5) heat the substrate on hot plate at 150 °C for 5 min, and (6) soak the substrates in acetone to dissolve resists and lift-off the material outside the patterns.

(75 W, 50 sccm flow rate, 75 mTorr operating pressure). The purpose of plasma treatment is to not only remove any undeveloped resist in the patterned areas but also to increase the hydrophilicity of PMMA surface.[28] This is necessary to improve the wettability and effective filling of the patterned areas by solutions. The plasma-treated patterned substrates were used immediately for spin-coating solutions. The solutions were spun between 3000 and 6000 rpm for 45 s and were heated immediately on a hot plate for 10 min at 150 °C. The substrates were soaked subsequently in acetone to dissolve resists, lift-off material outside the patterned areas, and generate solid structures with controlled dimensions. The essence of the scheme is thus using patterned e-beam resists as molds to define the location and size of nanostructures.

To demonstrate the capabilities of the scheme, we have initially employed solutions of technologically important inorganic ceramic oxides such as ZnO and PZT. Figure 2 shows scanning electron microscope (SEM) images of ZnO patterns made using soft eBL process on (100) Si substrates with 600-nm-thick thermal oxide. ZnO sol is prepared using chemicals purchased from Sigma-Aldrich and used in as-received form without further purification. In a typical process, zinc oxide sol is prepared by stirring a mixture of zinc acetate dihydrate, 2-methoxy ethanol, and ethanol amine at 60 °C for 2 h. The relative compositions were adjusted to give a 0.1 M ZnO sol with equimolar ratio of zinc and ethanol amine. This sol is transparent and has remained stable for more than a year in prior experiments. The patterns in Figure 2 were imaged after annealing them in air for 20 min at 700 °C to remove most of the organic material. The inset in Figure 2a shows the line width to be about 40 nm and spacing between lines of about 600 nm, demonstrating the high resolution and high spatial density achievable by this scheme. In addition, it is interesting that ZnO lines as narrow

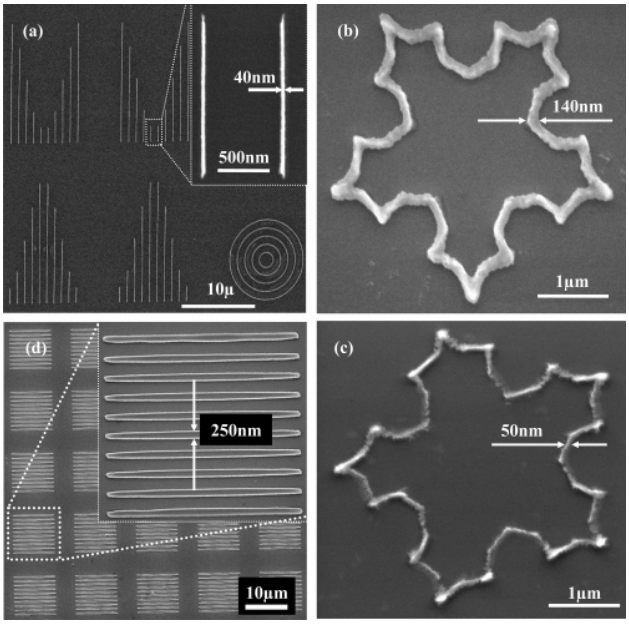

Figure 2. (a) Backscattered electron (BSE) image of ZnO patterns on SiO_x substrates annealed in air at 700 °C for 20 min, (b) secondary electron (SE) image before annealing, (c) SE image after annealing at 700 °C for 20 min in air, and (d) SE image of annealed patterns over a large area.

as 40 nm are continuous over 15-μm length even after annealing at 700 °C. The effect of annealing on line dimensions can be inferred from Figure 2b and c. These two images show that line widths decrease by nearly 70% upon annealing in air at 700 °C for 20 min due primarily to combustion of organics. From atomic force microscope (AFM) measurements (not shown here), we noticed that the height of the lines shrinks on average by about 50% after

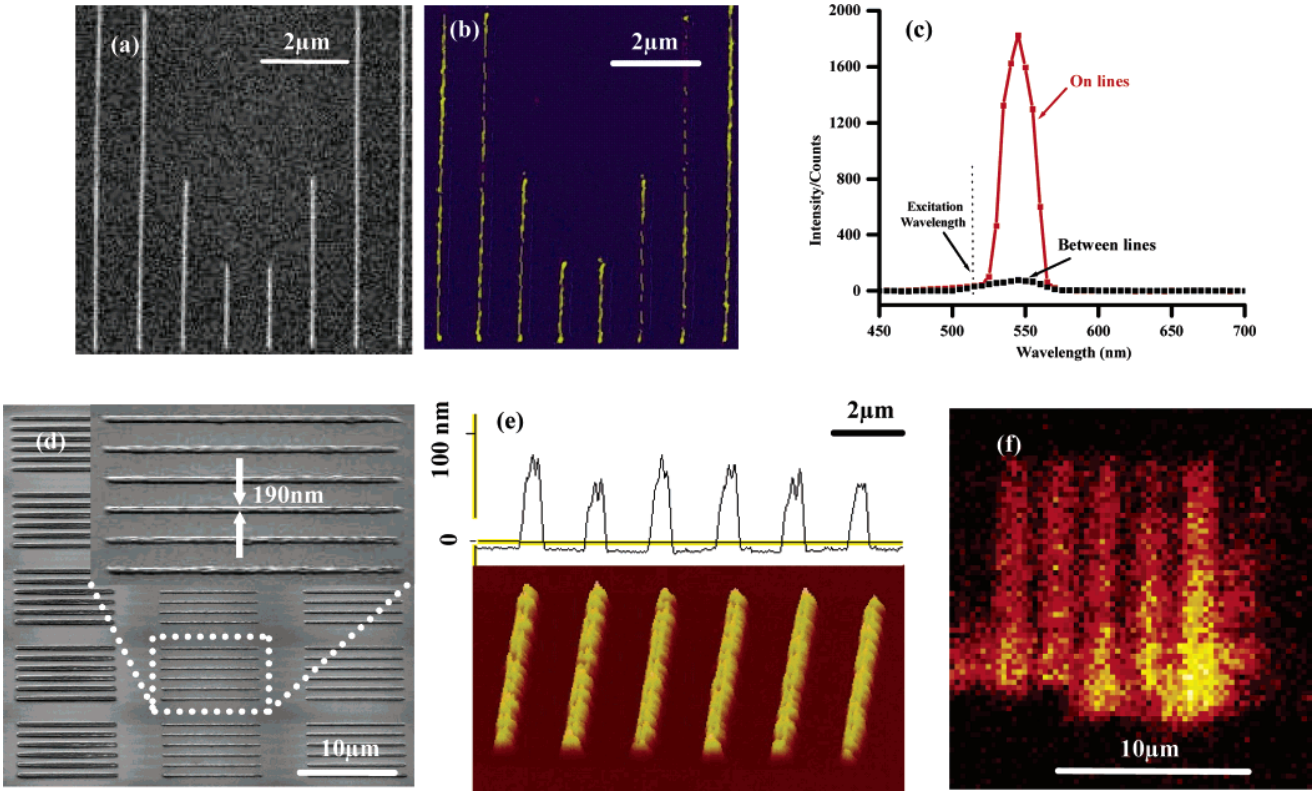

Figure 3. (a) Backscattered electron image of ZnO patterns on a SiO_x/Si substrate heated at 700 °C for 20 min in air. (b) Photoluminescence (PL) image of the patterns shown in part a collected in illumination mode using NSOM operating in constant height-mode to decouple cross-talk from topography. (c) PL spectra collected on and between ZnO lines. (d) SEM image of polypyrrole patterns on a SiO_x/Si substrate. (e) Topographic AFM image (tapping mode) and cross-sectional profile of the polypyrrole patterns. (f) CN^- ion map taken using SIMS. These images were not taken from same locations.

this annealing step from 200 to about 100 nm. Taking into account only the shrinkage in width and height of a typical line pattern, these values translate to about 85% volume shrinkage. Despite such large volume changes, the lines remain continuous over the entire length indicating perhaps that these lines might contain high nanoscale porosity, which is well known in ceramic thin films prepared via sol−gel route.[29] This could prove very valuable for their sensor and catalytic applications. Such large shrinkages have also been reported earlier for several ceramic structures fabricated using other patterning techniques, and in some cases such large shrinkages were reported to have given rise to significant feature distortion.[30,31] Figure 2d shows a scanning electron microscope (SEM) image of 250-nm-wide and 10-μm-long ZnO lines patterned on the same substrate and after annealing at the same conditions. This demonstrates the reproducibility of patterns over large areas with high spatial density using this approach. From the inset in Figure 2d, it can be noticed that sol segregates to the edges of the pattern with a trough in the middle of each line. This is the effect of spin coating similar to the surface contour of liquid in a spinning beaker. We have noticed that lower spinning speeds give rise to shallower troughs for a given line-width (i.e., larger line-widths result in a more dramatic 'beaker-effect"). However, too low spinning speeds will result in poor lift-off. Thus, there is a minimum spinning speed for a given pattern density to get effective lift-off. The patterns in Figure 2 were obtained by spin coating at 6000 rpm.

To further confirm the chemical identity of the patterns, we investigated the functionality of the patterns. Figure 3a shows the backscattered electron (BSE) image of ZnO patterns annealed at 700 °C in air for 20 min, whereas Figure 3b shows the photoluminescence (PL) image of these patterns collected using near-field scanning optical microscopy (NSOM) (MultiView 100, Nanonics Imaging Ltd). The PL image was collected in illumination mode using a 50-nm-diameter tip operating in constant-height mode to decouple the cross talk from the topography signal.[32−34] The patterns were excited using an Ar ion laser (λ = 514.5 nm, 10 mW output power), and the source signal was filtered from the PL signal using a 520-nm long-pass filter. The emitted signal is then fed into a Triax 180 monochromator and subsequently to an avalanche-photodiode (APD). Thus, the optical image in Figure 3b unambiguously shows the defect-induced emission from ZnO lines and confirms the identity of the patterns. The PL spectra collected from the ZnO line and between the lines are shown in Figure 3c. The spectrum from the lines shows a strong peak at 544 nm, which is assigned to the defect-induced emission from ZnO.[35−37] As expected, this peak is absent when measured between the lines, although a small hump could be seen at this value that could be due to the proximity of the tip to the lines.

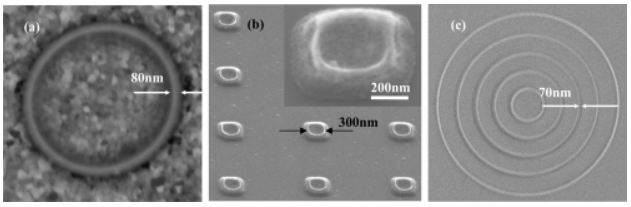

Figure 4. Versatility of the technique is demonstrated through patterning of different materials on different substrates. (a) PZT on Pt, (b) PZT on Nb/STO (inset shows the magnified view of one of the squares), and (c) ZnO on sapphire.

In a separate experiment, we patterned organic material using a dilute solution of polypyrrole, a popular conducting polymer, on a SiO_x/Si surface. Polypyrrole in 3% water was received as a black solution with proprietary organic acids from Sigma-Aldrich. This solution was further diluted to a 1:3 ratio of polypyrrole to water and was used for patterning. Figure 3d shows the SEM image of polypyrrole patterns with different line widths and spacing. The inset in this Figure shows a section of the pattern with 190-nm width. The 3D AFM topographic image and cross-sectional profile of a section of this pattern is shown in Figure 3e, indicating that the height of the lines is uniform. To confirm the chemical identity of these patterns, we took ion maps using a secondary ion mass spectrometer (SIMS). Figure 3f shows the SIMS CN^- ion maps of a section of the pattern, which is consistent with the presence of polypyrrole. The poorer resolution of the patterns in the SIMS ion map is due partly to coarser Ga ion probe size (~300 nm). This further validates that the soft eBL approach is applicable not only to inorganic solutions but also to organic solutions. The soft eBL approach would be extremely valuable for patterning polymers because, similar to ceramics etching, using polymers to generate nanostructures is otherwise very difficult.

We have further extended the soft eBL approach to diverse materials systems with a variety of substrates. Figure 4a shows 80-nm PZT ring structure patterned on a Pt/Ti/SiO_x/Si substrate. This substrate is well known to produce highly textured and device quality PZT films using the sol−gel route. Figure 4b shows 500-nm-wide PZT square patterns on a Nb doped strontium titanate (Nb/STO) single-crystal substrate. Transparent and highly stable 0.1 M PZT sol was prepared following a recipe reported elsewhere.[38,39] The patterns in Figure 4a and b were annealed at 600 °C for 2 h in air. The height difference at the edges of the square patterns in Figure 4b is a result of undercut due to higher sensitivity of the copolymer compared to PMMA. The effect of undercut is more prominent in these patterns because we have used relatively high doses (2 nC/cm) compared to other patterns in this work. Figure 4c shows ZnO patterns on another technologically important substrate, sapphire. Although the substrates in Figure 4a and b are electrical conductors, sapphire is an insulating material making eBL almost impossible because of severe charging effects. However, we are able to pattern on the sapphire substrate by backfilling the chamber with water vapor to 1 Torr chamber pressure to minimize the charging effects.[40] The different substrates in Figure 4 are chosen as representative for different classes of materials: polycrystal, single-crystal, insulating, and conducting. Through these results, we demonstrate the applicability of this scheme to a wide selection of substrate-material systems and highlight the remarkable versatility of the soft eBL approach. These results are particularly interesting from the point of obtaining ceramic nanostructures and possibly single-crystalline structures with a known epitaxial relationship to the appropriate substrate[41−44] and ultimately enabling one to engineer the microstructure of the nanopatterns through a careful choice of substrate and annealing scheme.

Although developing patterning techniques is important, one of the primary goals of patterning is to fabricate miniaturized devices. Here we demonstrate one such example through the fabrication of ZnO nanostructures and probing their UV photosensing properties. Figure 5a shows a SEM image of 75-nm-wide ZnO lines patterned using this scheme across gold electrodes with a 10-μm gap. The gold electrodes were fabricated previously on a SiO_x/Si substrate using conventional photolithography. The electrodes consist of 30-nm Au on top of 5-nm Ti deposited by an e-beam evaporation technique. The ZnO lines in Figure 5a were heated only at 150 °C for 10 min and therefore are not likely to be crystalline. The AFM cross-sectional profile of these lines measured on Au electrodes is shown in Figure 5b. The ZnO patterns were found to be highly resistive in room light, whereas their resistance decreased by 3 to 4 orders of magnitude when they were exposed to 254-nm light. All of the electrical measurements were performed at room temperature. The current−voltage ($I-V$) curve of ZnO patterns when exposed to 254-nm light is shown in Figure 5c. At a 5 V bias, the resistivity of each line under 254-nm light is about 6 MΩ cm. The current modulation upon exposure to 254-nm UV light in air is shown in Figure 5d. When ZnO is exposed to light with λ greater than the band gap (~385 nm), electrons are excited to the conduction band, increasing the electrical conductivity. In addition, the conductivity could also increase because of the desorption of oxygen from surface and concomitant electron donation to the ZnO matrix.[45,46] It is remarkable that both the response and recovery time are about 2 s, which is comparable to the performance of ZnO nanowires.[46] This is even more interesting because unlike nanowires, these ZnO patterns are not crystalline, suggesting that high crystallinity is not a prerequisite for superior performance of ZnO nanostructures for photodetector applications. Although their performance should be thoroughly evaluated for long-term stability, this result nevertheless demonstrates the high performance capability of ZnO nanostructures prepared using this scheme.

We have demonstrated a versatile nanopatterning approach suitable for a broad range of material−substrate systems. There are several advantages to this approach. First, the types of materials that can be patterned seem to be limited only by the availability of appropriate solution precursors that are compatible with e-beam resists, such as ceramic and polymer solutions. Second, because of the use of highly sensitive e-beam resists such as PMMA for patterning, there is a distinct advantage over the "direct-write" eBL of e-beam

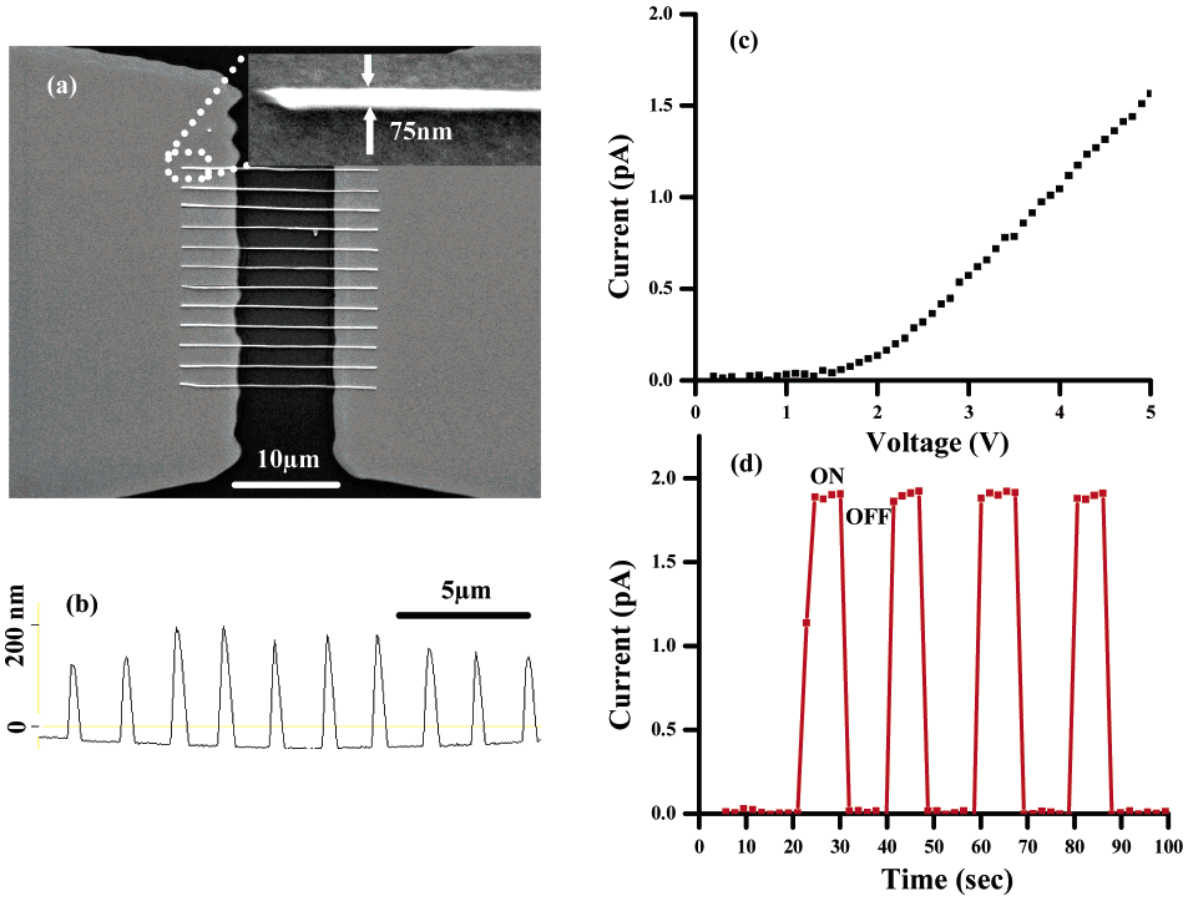

Figure 5. (a) SEM image (b) AFM cross-sectional profile of 75-nm-wide ZnO lines patterned across 10-μm gap Au electrodes. The lines were heated at 150 °C for 10 min in air. (c) $I-V$ curve of ZnO patterns when exposed to 254-nm light. (d) Conductivity modulation of these lines upon exposure to 254-nm UV light with 0.3 mW/cm^2 intensity. The current was monitored with a 5 V bias and measurements were taken at 2-s intervals. Response and recovery times are about 2 s.

sensitive inorganic resists[23] that typically require high electron doses, which translates into lower patterning speeds. In addition, spin coating is not only a low-cost process but also a high-throughput process. Last, by spinning the solution, we eliminate the need for any subsequent etching steps that might be undesirable, especially for ceramics and organic materials. There is a prior report by Shimada et al.[47] who have demonstrated a scheme to pattern nanostructures of ferroelectrics combining eBL and solution precursors, similar to this work. However, their scheme required etching ferroelectric material before dissolving e-beam resist. Recently, Xia et al.[48,49] have also reported patterning nanostructures of silica particles using interference lithography and spin coating. Thus, combining a high-resolution patterning technique such as eBL with a low-cost process such as spin coating has considerable potential for generating nanostructures using not only a solution precursor but also colloidal solutions.

In summary, we have presented a highly versatile nanopatterning approach for fabricating a variety of ceramic and organic nanostructures with controlled dimensions and locations termed as soft-eBL. The approach synergistically combines the advantages of e-beam lithography and wet chemistry. The chemical identity and functionality of fabricated nanostructures is demonstrated through a combination of analytical and measurement techniques such as SIMS, NSOM, and UV sensor performance. In addition, we propose extending the approach presented in this report to other high-resolution patterning techniques such as nanoimprint lithography in order to harness the additional advantage of high throughputs.

Acknowledgment. We acknowledge the Nanoscale Science and Engineering Initiative of the National Science Foundation (under NSF award no. EEC-0118025) and the U.S. Department of Energy (DOE-BES) for support of this research. This work was performed in the NIFTI and EPIC facilities of NUANCE Center at Northwestern University. NUANCE Center is supported by NSF-NSEC, NSF-MRSEC, Keck Foundation, the state of Illinois, and Northwestern University.

References

(1) Lakeman, C. D. E.; Payne, D. A. *Mater. Chem. Phys.* **1994**, *38*, 305.
(2) Martin, C. R.; Aksay, I. A. *J. Electroceram.* **2004**, *12*, 53.
(3) Kolmakov, A.; Moskovits, M. *Annu. Rev. Mater. Res.* **2004**, *34*, 151.
(4) Look, D. C. *Mater. Sci. Eng., B* **2001**, *80*, 383.
(5) Yun, M. H.; Myung, N. V.; Vasquez, R. P.; Lee, C. S.; Menke, E.; Penner, R. M. *Nano Lett.* **2004**, *4*, 419.
(6) Mohaddes-Ardabili, L.; Zheng, H.; Ogale, S. B.; Hannoyer, B.; Tian, W.; Wang, J.; Lofland, S. E.; Shinde, S. R.; Zhao, T.; Jia, Y.; Salamanca-Riba, L.; Schlom, D. G.; Wuttig, M.; Ramesh, R. *Nat. Mater.* **2004**, *3*, 533.

(7) Nagarajan, V.; Ganpule, C. S.; Ramesh, R. *Ferroelectr. Random Access Mem.* **2004**, *93*, 47.
(8) Chae, G. S. *Jpn. J. Appl. Phys., Part 1* **2001**, *40*, 1282.
(9) Bagnall, D. M.; Chen, Y. F.; Zhu, Z.; Yao, T.; Koyama, S.; Shen, M. Y.; Goto, T. *Appl. Phys. Lett.* **1997**, *70*, 2230.
(10) Tang, Z. K.; Wong, G. K. L., Yu, P.; Kawasaki, M.; Ohtomo, A.; Koinuma, H.; Segawa, Y. *Appl. Phys. Lett.* **1998**, *72*, 3270.
(11) Buhlmann, S.; Dwir, B.; Baborowski, J.; Muralt, P. *Appl. Phys. Lett.* **2002**, *80*, 3195.
(12) Alexe, M.; Harnagea, C.; Hesse, D. *J. Electroceram.* **2004**, *12*, 69.
(13) Zheng, H.; Wang, J.; Lofland, S. E.; Ma, Z.; Mohaddes-Ardabili, L.; Zhao, T.; Salamanca-Riba, L.; Shinde, S. R.; Ogale, S. B.; Bai, F.; Viehland, D.; Jia, Y.; Schlom, D. G.; Wuttig, M.; Roytburd, A.; Ramesh, R. *Science* **2004**, *303*, 661.
(14) Moshnyaga, V.; Damaschke, B.; Shapoval, O.; Belenchuk, A.; Faupel, J.; Lebedev, O. I.; Verbeeck, J.; Van Tendeloo, G.; Mucksch, M.; Tsurkan, V.; Tidecks, R.; Samwer, K. *Nat. Mater.* **2003**, *2*, 247.
(15) Chou, S. Y.; Krauss, P. R.; Renstrom, P. J. *Science* **1996**, *272*, 85.
(16) Su, M.; Liu, X. G.; Li, S. Y.; Dravid, V. P.; Mirkin, C. A. *J. Am. Chem. Soc.* **2002**, *124*, 1560.
(17) Piner, R. D.; Zhu, J.; Xu, F.; Hong, S. H.; Mirkin, C. A. *Science* **1999**, *283*, 661.
(18) Tang, Q.; Shi, S. Q.; Zhou, L. M. *J. Nanosci. Nanotechnol.* **2004**, *4*, 948.
(19) Zhang, L. B.; Shi, J. X.; Yuan, J. L.; Ji, S. M.; Chang, M. *Adv. Mater. Manuf. Sci. Technol.* **2004**, *471*−*472*, 353.
(20) Ginger, D. S.; Zhang, H.; Mirkin, C. A. *Angew. Chem., Int. Ed.* **2004**, *43*, 30.
(21) Payne, D. A.; Clem, P. G. *J. Electroceram.* **1999**, *3*, 163.
(22) Auger, M. A.; Schilardi, P. L.; Caretti, I.; Sanchez, O.; Benitez, G.; Albella, J. M.; Gugo, R.; Fonticelli, M.; Vazquez, L.; Salvarezza, R. C.; Azzaroni, O. *Small* **2005**, *1*, 300.
(23) Saifullah, M. S. M.; Subramanian, K. R. V.; Tapley, E.; Kang, D. J.; Welland, M. E.; Butler, M. *Nano Lett.* **2003**, *3*, 1587.
(24) Heule, M.; Schell, J.; Gauckler, L. J. *J. Am. Ceram. Soc.* **2003**, *86*, 407.
(25) Kim, E.; Xia, Y.; Whitesides, G. M. *J. Am. Chem. Soc.* **1996**, *118*, 5722.
(26) Gratson, G. M.; Xu, M. J.; Lewis, J. A. *Nature* **2004**, *428*, 386.
(27) Lewis, J. A.; Gratson, G. M. *Mater. Today* **2004**, 32.
(28) Chai, J. N.; Lu, F. Z.; Li, B. M.; Kwok, D. Y. *Langmuir* **2004**, *20*, 10919.
(29) Brinker, C. J.; Sehgal, R.; Hietala, S. L.; Deshpande, R.; Smith, D. M.; Loy, D.; Ashley, C. S. *J. Membr. Sci.* **1994**, *94*, 85.
(30) Seraji, S.; Wu, Y.; Jewell-Larson, N. E.; Forbess, M. J.; Limmer, S. J.; Chou, T. P.; Cao, G. Z. *Adv. Mater.* **2000**, *12*, 1421.
(31) Martin, C. R.; Aksay, I. A. *J. Phys. Chem. B* **2003**, *107*, 4261.
(32) Donthu, S. K.; Pan, Z.; Shekhawat, G. S.; Dravid, V. P.; Balakrisnan, B.; Tripathy, S. *J. Appl. Phys.*, in press.
(33) Carminati, R.; Madrazo, A.; NietoVesperinas, M.; Greffet, J. J. *J. Appl. Phys.* **1997**, *82*, 501.
(34) Hecht, B.; Bielefeldt, H.; Inouye, Y.; Pohl, D. W.; Novotny, L. *J. Appl. Phys.* **1997**, *81*, 2492.
(35) Aoki, T.; Hatanaka, Y.; Look, D. C. *Appl. Phys. Lett.* **2000**, *76*, 3257.
(36) Zhang, S. B.; Wei, S.-H.; Zunger, A. *Phys. Rev. B* **2001**, *63*, 75205.
(37) Choopun, S.; Vispute, R. D.; Noch, W.; Balsamo, A.; Sharma, R. P.; Venkatesan, T.; Iliadis, A.; Look, D. C. *Appl. Phys. Lett.* **1999**, *75*, 3947.
(38) Kim, D. J.; Maria, J. P.; Kingon, A. I.; Streiffer, S. K. *J. Appl. Phys.* **2003**, *93*, 5568.
(39) Kim, S. H.; Kim, D. J.; Streiffer, S. K.; Kingon, A. I. *J. Mater. Res.* **1999**, *14*, 2476.
(40) Myers, B. D.; Dravid, V. P. Direct Patterning of nanometer-scale structures on insulating substrates using variable pressure electron beam lithography (VP-eBL). In *Proceedings of Microscopy and Microanalysis*, 2005; in press.
(41) Andeen, D.; Loeffler, L.; Padture, N.; Lange, F. F. *J. Cryst. Growth* **2003**, *259*, 103.
(42) Lange, F. F.; Goh, G. K. L. *J. Ceram. Process Res.* **2001**, *2*, 4.
(43) Lange, F. F. *Science* **1996**, *273*, 903.
(44) Brinker, C. J. *Curr. Opin. Colloid Interface Sci.* **1998**, *3*, 166.
(45) Takahashi, Y.; Kanamori, M.; Kondoh, A.; Minoura, H.; Ohya, Y. *Jpn. J. Appl. Phys. 1* **1994**, *33*, 6611.
(46) Kind, H.; Yan, H. Q.; Messer, B.; Law, M.; Yang, P. D. *Adv. Mater.* **2002**, *14*, 158.
(47) Shimada, S.; Hirano, S.; Kuwabara, M. *Jpn. J. Appl. Phys., Part 1* **2003**, *42*, 6721.
(48) Xia, D. Y.; Biswas, A.; Li, D.; Brueck, S. R. J. *Adv. Mater.* **2004**, *16*, 1427.
(49) Xia, D. Y.; Brueck, S. R. J. *Nano Lett.* **2004**, *4*, 1295.

NL050954T